Nuclear Overhauser Effect Studies of the Conformations and Binding Site Environments of Deoxynucleoside Triphosphate Substrates Bound to DNA Polymerase I and Its Large Fragment†

Lance J. Ferrin and Albert S. Mildvan*

Department of Biological Chemistry, Johns Hopkins University School of Medicine, Baltimore, Maryland 21205

Received April 4, 1985

ABSTRACT: The conformations and binding site environments of Mg^{2+}TTP and Mg^{2+}dATP bound to *Escherichia coli* DNA polymerase I and its large (Klenow) fragment have been investigated by proton NMR. The effect of the large fragment of Pol I on the NMR line widths of the protons of Mg^{2+}TTP detected one binding site for this substrate with a dissociation constant of 300 ± 100 μM and established simple competitive binding of deoxynucleoside triphosphates at this site in accord with previous equilibrium dialysis experiments with whole Pol I [Englund, P. T., Huberman, J. A., Jovin, T. M., & Kornberg, A. (1969) *J. Biol. Chem. 244*, 3038]. Primary negative nuclear Overhauser effects were used to calculate interproton distances on enzyme-bound Mg^{2+}dATP and Mg^{2+}TTP. These distances established that each substrate was bound with an anti-glycosidic torsional angle (χ) of 50 ± 10° for Mg^{2+}dATP and 40 ± 10° for Mg^{2+}TTP. The sugar pucker of both substrates was predominantly O1′-endo, with a C5′–C4′–C3′–O3′ exocyclic torsional angle (δ) of 95 ± 10° for Mg^{2+}dATP and 100 ± 10° for Mg^{2+}TTP. The consistency of these conformations with those previously proposed, on the basis of distances from Mn^{2+} at the active site [Sloan, D. L., Loeb, L. A., Mildvan, A. S., & Feldman, R. J. (1975) *J. Biol. Chem. 250*, 8913], indicates a unique conformation for each bound nucleotide. The χ and δ values of the bound substrates are appropriate for nucleotide units of B DNA. Intermolecular Overhauser effects observed on substrate protons upon preirradiation of enzyme protons established substrate proximity ($\lesssim$5 Å) to at least two hydrophobic amino acids (Ile, Leu, or Val) and to an aromatic amino acid.

Although DNA polymerase I (Pol I)[1] from *Escherichia coli* has been extensively studied (Kornberg, 1980, 1982), the detailed mechanism by which this enzyme catalyzes the accurate copying of DNA remains obscure. With Mg^{2+} or Mn^{2+} as the divalent cation activator, Pol I catalyzes nucleophilic substitution on the α-P of deoxynucleoside triphosphates, by the 3′-hydroxyl terminus of the primer chain, with pyrophosphate as the leaving group. The elongation of the primer takes place in a manner consistent with Watson–Crick base pairing between the incoming deoxynucleoside triphosphate and the template. In addition to this polymerizing activity, the enzyme also possesses 3′–5′ and 5′–3′ exonuclease activities. Treatment of this 103 000-dalton polypeptide with subtilisin generates two fragments; the larger fragment (Klenow fragment) of 68 000 daltons possesses the polymerizing and 3′–5′ exonuclease activities, while the smaller fragment of 35 000 daltons possesses the 5′–3′ exonuclease activity (Brutlag et al., 1969; Klenow & Henningsen, 1970).

Both whole Pol I and the large fragment have been cloned in high-expression vectors (Kelley & Stump, 1979; Joyce & Grindley, 1983), and in the case of the large fragment, the enzyme has been crystallized and an X-ray structure determined (Ollis et al., 1985), which also identified a monophosphate binding site. Structural information concerning deoxynucleoside triphosphates bound to Pol I was previously obtained by Sloan et al. (1975), who used nuclear magnetic resonance techniques to obtain distances from Mn^{2+}, a divalent paramagnetic activator, to the protons and phosphorus atoms of bound TTP and dATP. These early studies did not uniquely define the conformations of the bound substrates. In the present study, the nuclear Overhauser effect (NOE) has been used to determine interproton distances, and thereby the conformation of Mg^{2+}dATP and Mg^{2+}TTP bound to both whole Pol I and its large fragment, and to characterize the protein environment of the deoxynucleoside triphosphate binding site. Preliminary reports of this work have been published (Ferrin & Mildvan, 1984, 1985).

Experimental Procedures

Materials

Escherichia coli strain (CJ155), which overproduces the large fragment of DNA polymerase I, was generously provided by N. Grindley. The enzyme was purified from this strain by the method of Joyce & Grindley (1983), including their optional gel filtration step, and was assayed by the method of Setlow (1974) with poly(dAT) as template-primer and [^{3}H]dATP and TTP as substrates. The purified large fragment had a specific activity of 15 000 units/mg and was judged to be >99% pure by polyacrylamide gel electrophoresis. *E. coli* strain (CM5199), which overproduces whole DNA polymerase I, was generously provided by W. Brown of Carnegie-Mellon University, Pittsburgh, PA. The enzyme was pu-

† This work was supported by National Institutes of Health Grant AM28616 and National Science Foundation Grant PCM8219464. L.J.F. is an awardee of the Medical Scientist Training Program (5T32GM07309).

[1] Abbreviations: Pol I, *Escherichia coli* DNA polymerase I; NOE, nuclear Overhauser effect; PEI, poly(ethylenimine); pH*, meter reading in ^2H_2O; A/D, analog to digital conversion; DSS, sodium 4,4-dimethyl-4-silapentanesulfonate; FID, free induction decay; EDTA, ethylenediaminetetraacetic acid; Tris-HCl, tris(hydroxymethyl)aminomethane hydrochloride.

0006-2960/85/0424-6904$01.50/0

rified by a modification (Ferrin et al., 1983) of the method of Kelley & Stump (1979). The purified Pol I had a specific activity of 6200 units/mg and was judged to be 91% pure by polyacrylamide gel electrophoresis.

All nucleotides were purchased from P-L Biochemicals. PEI–cellulose plates were purchased from J. T. Baker. Chelex-100 was purchased from Bio-Rad and was converted to the K^+ form before use. Ultrapure $MgCl_2$ was purchased from Accurate Chemical & Scientific Corp.; 99.96% ^2H_2O was purchased from Wilmad, and 99.8% ^2H_2O was purchased from Stohler and was sublimed under vacuum to remove a small amount of a white amorphous impurity.

Methods

The concentration of the large fragment was determined spectrophotometrically by using $A_{280}^{1\%} = 9.3$ (Setlow et al., 1972) and a M_r of 68 000 (Joyce et al., 1982). The concentration of whole Pol I was determined by using $A_{280}^{1\%} = 8.5$ (Jovin et al., 1969) or by the method of Lowry et al. (1951) with bovine plasma albumin as the standard. A factor of 0.80 was found to be necessary to relate Lowry values to absolute polymerase concentrations determined spectrophotometrically. A M_r of 103 000 was assumed (Joyce et al., 1982).

To remove trace metal contaminants (Ferrin et al., 1983) prior to each NMR experiment, the enzyme solution was passed down a 1.3 × 20 cm column of Sephadex G-25, which had been washed with 10 mM EDTA and equilibrated with 10 mM Tris-HCl, pH 7.50, and 32 mM KCl. The fractions containing protein were pooled to approximately 3-mL total volume. The pool was then concentrated to 0.5 mL either by vacuum dialysis in a Schleicher & Schuell nitrocellulose collodion bag for whole Pol I or with a Millipore CX-10 ultrafiltration unit for the large fragment. The concentrated enzyme was then diluted to 3 mL with deuterated 10 mM Tris-HCl, pH* 7.10, and 32 mM KCl in ^2H_2O and concentrated again. This process was repeated until the enzyme had been deuterated and concentrated a total of 4 times. The enzyme solution was then lyophilized to dryness and redissolved in 99.96% ^2H_2O (Wilmad). The specific activities of the enzymes were unaffected at the end of these manipulations or during the subsequent NMR experiments. The concentration of either enzyme in the NMR experiments was generally 0.14 mM, but concentrations as high as 0.38 mM did not detectably alter the results. In the NMR experiments, nucleotides were present in a 20-fold molar excess over enzyme, but increasing the ratio to 40 gave indistinguishable results.

The concentrations of TTP, dATP, and dGTP were determined spectrophotometrically by using $\epsilon_{267} = 9.6 \times 10^3\ M^{-1}$, $\epsilon_{259} = 15.2 \times 10^3\ M^{-1}$, and $\epsilon_{253} = 13.7 \times 10^3\ M^{-1}$, respectively. Since Englund et al. (1969) found that deoxynucleoside triphosphatase activities were present as trace contaminants in even their highly purified Pol I preparations, the intactness of the triphosphates was measured at the end of each NMR experiment by thin-layer chromatography on PEI–cellulose plates developed in 1.0 M LiCl, pH 7.0. With the large fragment of Pol I, in no case did the breakdown of triphosphates exceed ~20%, even after 10 days at 24 °C. However, in the case of whole Pol I, a 30–40% breakdown of dATP to dADP and dAMP was observed after 4 days at 24 °C. In all cases, the conformational studies of the enzyme-bound nucleotides, which are the most sensitive to the purity of the triphosphate, were done when the extent of breakdown was ≤10% with the large fragment and ≤20% with whole Pol I.

All NMR experiments were carried out in deuterated 10 mM Tris-HCl, pH* 7.10, and 32 mM KCl at 24 °C. All NMR solutions excluding those containing only enzyme or Mg^{2+} were passed through Chelex-100 prior to deuteration to remove trace metal impurities. The concentration of free Mg^{2+} necessary for optimal activity of whole Pol I was found by Travaglini et al. (1975) to range from 0.3 to 2.0 mM, depending on the template-primer system used. Repetition of their study with the large fragment of Pol I in 10 mM Tris-HCl, pH 7.50, 32 mM KCl, and poly(dAT) as template-primer showed an almost identical dependence of activity on free Mg^{2+}. Accordingly, most of the NMR experiments were carried out with a Mg^{2+} concentration 0.3 mM in excess of the nucleotide concentration (2.7–3.1 mM). Under these conditions, from the dissociation constant of 0.1 mM (Kerson et al., 1967) the free Mg^{2+} was 0.7 mM. NMR experiments done in absence of template at variable Mg^{2+} concentrations showed the conformation of enzyme-bound dATP to be independent of the concentration of free Mg^{2+} over the range of 0.7–10 mM.

NMR Spectroscopy. The equipment and pulse sequences used were essentially those of Rosevear et al. (1983). The ^1H NMR spectra were collected on a Bruker WM 250 NMR spectrometer equipped with an Aspect 2000 A computer using 16-bit A/D conversion, quadrature phase detection and a 90° observation pulse. Chemical shifts are expressed relative to external DSS. The time dependence of the nuclear Overhauser effect was measured with the interleaved pulse sequence:

$$[[\text{RD–preirradiate } (t,\omega_1)\text{–observation pulse}]_{8\text{or}16}\text{–}[\text{RD–preirradiate } (t, \omega_{\text{off-res}})\text{–observation pulse}]_{8\text{or}16}\text{–}[\text{RD–preirradiate } (t, \omega_2)\text{–observation pulse}]_{8\text{or}16}]_n$$

where RD is the relaxation delay ($\geq 5T_1$), t is the duration of preirradiation, and ω_1 and ω_2 are the frequencies of the irradiated resonances. This pulse sequence measures the truncated driven NOE (Wagner & Wuthrich, 1979), which is especially useful in measuring the initial buildup rates of NOE's, minimizing the effects of spin–diffusion, and thereby clearly distinguishes primary from higher order NOE's (Rosevear et al., 1983). Sufficient free induction decays (FID's), typically 256, were collected to determine the magnitude of the NOE to ±0.5% of a single proton intensity, as estimated by integration of both the difference spectra and the control spectra. Integration did not alter the magnitudes of the NOE's but decreased their errors.

The proton decoupler was utilized to produce the selective preirradiation pulse of duration t, between 0.05 and 2.0 s, and a pulse power of 10 μW was typically used in determining the conformation of the enzyme-bound nucleotides. A pulse power of 20 μW for 1.0 s was used in obtaining the "action spectra" of NOE's from protein to nucleotide resonances. NOE's on free nucleotides in the absence of enzyme were measured with pulse powers of 0.6 and 2 mW. The NOE's were observed from the Fourier transform of the difference spectra obtained by subtraction of the control FID's ($\omega_{\text{off-res}}$) from experimental FID's (ω_1 or ω_2). $\omega_{\text{off-res}}$ was at 9.4 ppm, an empty region of the spectrum.

The presence of enzyme did not alter the chemical shifts of any of the nucleotide resonances. The deoxyribose H3′ resonances of dATP and TTP, however, were partially or completely obscured by the HDO signal. The chemical shift of the H3′ resonance was determined by searching for a frequency that, upon continuous irradiation, decoupled the H3′ resonance from those of the H2′ and H2″. This frequency was independently confirmed by searching for a frequency that optimized the magnitude of the NOE's from H3′ to H2′ and H1′.

Longitudinal relaxation rates ($1/T_1$) were measured by a selective saturation–recovery method (Rosevear et al., 1983). Transverse relaxation rates ($1/T_2$) were calculated from the line width at half-height ($\Delta\nu$) by using the relation $1/T_2 = \pi\Delta\nu$.

NOE Data Reduction. The cross-relaxation rate (σ_{AB}) for the transfer of energy to spin A upon irradiation of spin B was calculated by using eq 1, in which $f_A(B)_t$ is the NOE to spin

$$f_A(B)_t = \frac{\sigma_{AB}}{\rho_A}(1 - e^{-\rho_A t}) + \frac{\sigma_{AB}}{\rho_A - c}(e^{-\rho_A t} - e^{-ct}) \quad (1)$$

A upon preirradiation of spin B for time t, ρ_A is the spin–lattice relaxation rate of spin A, and c is the rate constant for saturation of spin B, which accounts for the small lag period before the NOE's begin to build up.

Equation 1 describes the time dependence of the NOE for direct energy transfer between two isolated spins. Such effects are termed primary NOE's and are rarely observed if the distance between the two spins exceeds 4 Å. In some cases, however, energy may be serially transferred through several spins, leading to secondary and higher order NOE's between spins that are physically remote. Secondary effects require more time to develop than primary effects, so that the time dependence of the NOE can be used to identify the primary effect. In the present study, the time dependence of each effect was thoroughly determined.

The σ_{AB} values that involve the irradiation of the two superimposed H5′ and H5″ resonances of dATP and TTP or the three superimposed T-H5 methyl resonances have been divided by a factor of 2 or 3, respectively, to obtain the relevant σ_{AB} values for distance calculations (Noggle & Shirmer, 1971; Tropp, 1980).

Interproton distances (r_{AB}) were obtained from σ_{AB} by using eq 2, in which the constant $D = (\gamma^4\hbar^2/10)^{1/6} = 62.02$ Å $s^{-1/3}$,

$$r_{AB} = D[f(\tau_r)/\sigma_{AB}]^{1/6} \quad (2)$$

where γ is the proton gyromagnetic ratio and $f(\tau_r)$ is given by

$$f(\tau_r) = \frac{6\tau_r}{1 + 4\omega_I^2\tau_r^2} - \tau_r \quad (3)$$

where ω_I is the Larmor frequency and τ_r is the correlation time. The value of τ_r was calculated in each case from $\sigma_{H2''\rightarrow H1'}$ with eq 2 and the conformationally independent distance of 2.37 ± 0.10 Å between deoxyribose H2″ and H1′, based on model building and crystallographic studies (Levitt & Warshel, 1978). The upper limit of τ_r was estimated with eq 4 (Solomon, 1955) by using measured T_1/T_2 ratios of the nucleotide protons.

$$\frac{T_1}{T_2} = \frac{12\omega_I^4\tau_r^4 + 37\omega_I^2\tau_r^2 + 10}{16\omega_I^2\tau_r^2 + 10} \quad (4)$$

Determination of Absolute and Relative Dissociation Constants. In the presence of enzyme, the line widths of enzyme-bound substrate resonances as a function of substrate concentration were used to calculate dissociation constants, by essentially following the method of Schmidt et al. (1969). Under fast-exchange conditions, the observed line width of a substrate is the weighted average of the line widths for bound and unbound substrate. Titration curves of observed line width vs. substrate concentration were fit by iteratively varying the dissociation constant, and the line width for bound and unbound substrate. Similar plots of line widths of one substrate while titrating with a second substrate were used to obtain relative dissociation constants.

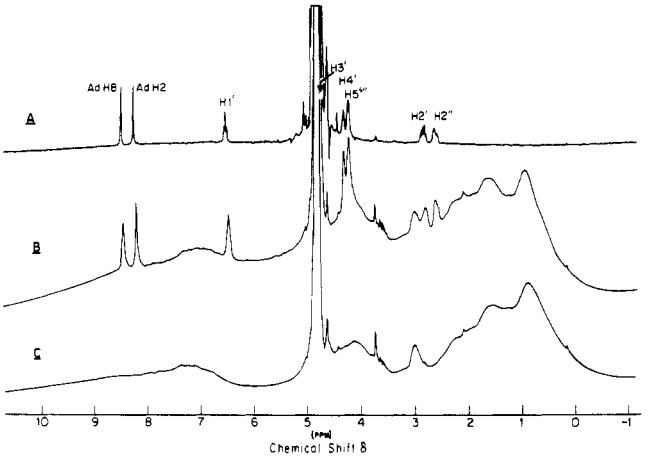

FIGURE 1: Proton NMR spectra of Mg^{2+}dATP in the absence and presence of the large fragment of Pol I. Spectrum A is of 6.1 mM dATP and 6.8 mM $MgCl_2$, which was acquired from 16 transients with a recycle time of 13 s. Spectrum B is of 17 mM dATP and 26 mM $MgCl_2$ in the presence of 0.38 mM large fragment. The spectrum was acquired from 64 transients with a recycle time of 5 s. Spectrum C is of 0.42 mM large fragment and 21 mM $MgCl_2$. The spectrum was acquired from 128 transients with a recycle time of 8 s. All samples contained 10 mM deuterated Tris-HCl buffer, pH* 7.1, and 32 mM KCl in ^2H_2O. T = 24 °C. NMR parameters: 3000-Hz spectral width, 16K time domain points, 16-bit A/D conversion, and 90° flip angle. A line broadening of 0.5 Hz was used.

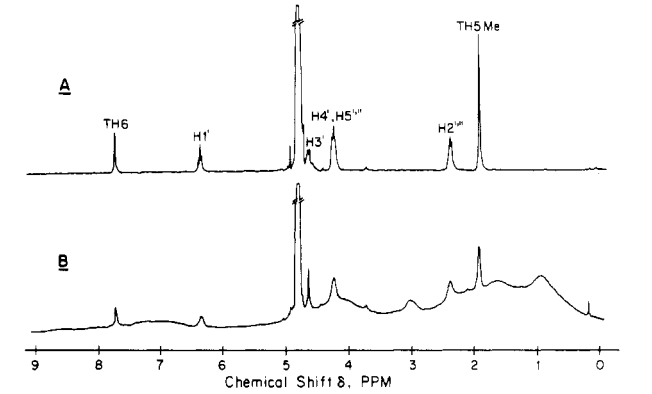

FIGURE 2: Proton NMR spectra of Mg^{2+}TTP in the absence and presence of the large fragment. Spectrum A is of 2.9 mM TTP and 3.2 mM $MgCl_2$. The spectrum was acquired from 64 transients with a recycle time of 13 s. Spectrum B is of 3.11 mM TTP and 3.41 mM $MgCl_2$ in the presence of 0.147 mM large fragment. The spectrum was acquired from 64 transients with a recycle time of 13 s. Experimental and NMR conditions were otherwise as described in Figure 1.

RESULTS

Diamagnetic Effects of the Large Fragment of Pol I on Relaxation Rates of Deoxynucleoside Triphosphates. As shown in Figure 1, the presence of the large fragment (0.38 mM) broadens the singlet H8 and H2 resonances of Mg^{2+}-dATP (17 mM) by 9 and 4 Hz, respectively. Comparable broadenings of the other resonances of Mg^{2+}dATP obscure their multiplet character. Similarly, the large fragment (0.15 mM) broadens the resonances of Mg^{2+}TTP (3.1 mM) by 6 Hz (Figure 2). The line broadenings of the substrate resonances by the enzyme were due to binding of the substrates rather than to an increase in viscosity, since they required the presence of Mg^{2+}, and the addition of Mg^{2+}dGTP reversed these effects. Such binding properties of deoxynucleoside triphosphate substrates to whole Pol I in the presence of Mg^{2+}

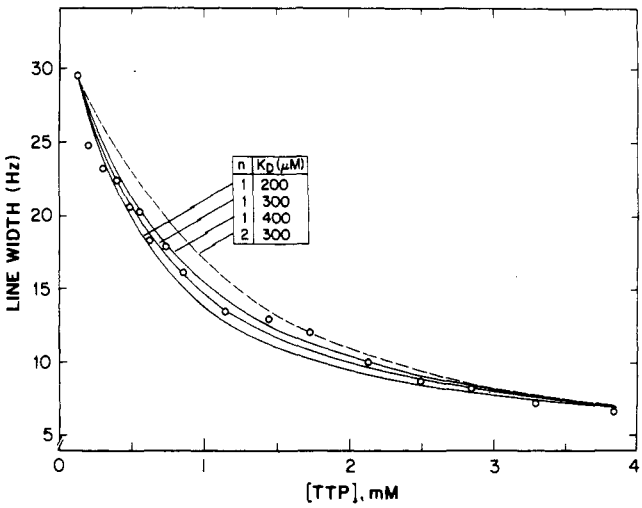

FIGURE 3: Effect of Mg^{2+}TTP concentration on the diamagnetic line broadening of the thymine H6 resonance by the large fragment. Line widths, measured at half-height, are accurate to within 7%. The solid lines were calculated as described under Experimental Procedures by assuming K_D's of 200, 300, and 400 μM for Mg^{2+}TTP binding to one site on the large fragment. The broken line was calculated by assuming a K_D of 300 μM for Mg^{2+}TTP binding to two equivalent sites on the large fragment. The sample contained 0.21 mM large fragment and 0.30 mM $MgCl_2$ in excess of the TTP concentration throughout the titration. The number of transients ranged from 20 000 to 1000, depending on the TTP concentration, with a recycle time of 1.8 s and 8K time domain points. All other experimental and NMR parameters were as described in Figure 1.

Table I: Comparison of Absolute and Relative Dissociation Constants of Deoxynucleotide Substrates from Pol I and Large Fragment

	NMR[a]		equilibrium dialysis[b]	
nucleotide	K_D(E–dNTP) (μM)	K_D(E–dNTP)/K_D(E–dGTP)	K_D(E–dNTP (μM)	K_D(E–dNTP)/K_D(E–dGTP)
TTP	300 ± 100	5.5 ± 1.5	81 ● 29	6.8 ± 3.0
dATP	270 ± 200[c]	5 ± 3	33 ± 8	2.8 ± 1.0
dGTP	54 ± 23[c]	1.0	12 ± 3	1.0

[a] Determined by line-width titrations of large fragment–substrate complexes at 0.3 mM Mg^{2+} in excess of nucleotide, 10 mM Tris-HCl, pH* 7.1, and 32 mM KCl in ^2H_2O. T = 24 °C. [b] Determined by Englund et al. (1969) for whole Pol I at 7 mM Mg^{2+}. [c] Not directly determined, but constrained to lie in this range based on the absolute and relative K_D's and their errors.

were previously demonstrated in equilibrium dialysis experiments (Englund et al., 1969).

The observed line width of the thymine H6 resonance of TTP in the presence of the large fragment as a function of TTP concentration is shown in Figure 3. Enzyme concentration was kept constant at 210 μM, and Mg^{2+} concentration was kept constant at 0.3 mM in excess of TTP concentration. The curve was fit, assuming that the observed line width was the weighted average between the free and bound species. Starting with the likely premise that there is one binding site per enzyme molecule, a dissociation constant, K_D, of 300 μM (Table I) fits the curve well, while 200 or 400 μM gives a poorer fit (Figure 3, solid lines). On the other hand, starting with the premise that there are two identical binding sites per enzyme molecule, a much poorer fit is obtained (dotted line).

The stoichiometry of one binding site per enzyme molecule was also found by equilibrium dialysis (Englund et al., 1969), although a (4 ± 2)-fold lower K_D was obtained (81 ± 29 μM), possibly due to the higher concentration of Mg^{2+} in the latter experiments.

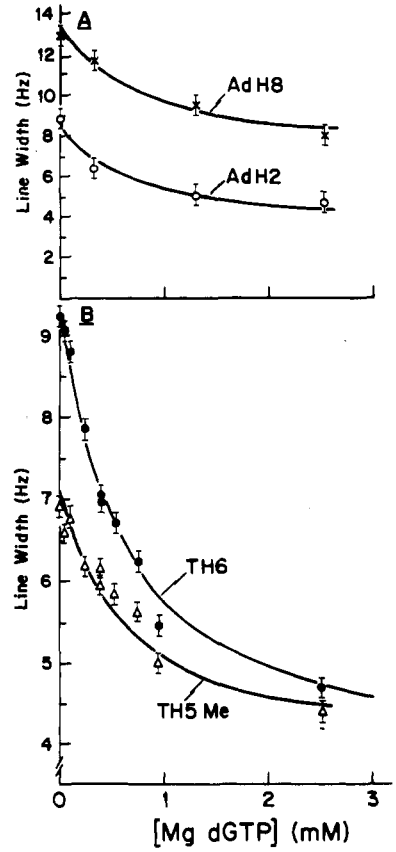

FIGURE 4: Effect of Mg^{2+}dGTP on the diamagnetic line broadening of the resonances of Mg^{2+}dATP and Mg^{2+}TTP. Samples of Mg^{2+}-dATP or Mg^{2+}TTP in the presence of the large fragment were titrated with concentrated solutions of Mg^{2+}dGTP. The concentration of Mg^{2+} in excess of nucleotide was maintained at 0.3 mM. The line widths, measured at half-height, were plotted as a function of the concentration of Mg^{2+}dGTP. The solid lines shown were calculated as under Experimental Procedures by assuming competitive binding at a single site on the large fragment with the relative K_D's listed in Table I. The small dilution (<10% or <20%) that occurred during the dATP or TTP titrations, respectively, was taken into account in the calculations. (A) Effect of Mg^{2+}dGTP on the line widths of Mg^{2+}dATP. The sample contained 2.75 mM dATP and 0.130 mM large fragment. The spectra were acquired with 256 transients with a recycle time of 7.7 s. (B) Effect of Mg^{2+}dGTP on the line widths of Mg^{2+}TTP. The sample contained 3.11 mM TTP and 0.147 mM large fragment. The spectra were acquired with 128 transients with a recycle time of 10.0 s. All other experimental and NMR parameters were as described in Figure 1.

Mutual Displacement of Deoxynucleoside Triphosphate Substrates from the Large Fragment. The renarrowing of broadened substrate resonances by a second substrate was used to measure the relative dissociation constants (K_D) of the large fragment–nucleotide complexes.

Solutions of the large fragment and Mg^{2+}dATP (Figure 4A) or Mg^{2+}TTP (Figure 4B) were titrated with small volumes of a concentrated solution of Mg^{2+}dGTP. As shown in Figure 4, as more Mg^{2+}dGTP was added, the line widths of the Mg^{2+}dATP and Mg^{2+}TTP resonances decreased. The experimental points were fit with theoretical curves (Figure 4), assuming that the nucleotides competitively bind to a single site and that the observed line broadening effect of the large fragment on Mg^{2+}dATP and Mg^{2+}TTP was proportional to occupancy of this site.

The ratios of the dissociation constants used to fit the titrations were 5 ± 3 for K_D(E–dATP)/K_D(E–dGTP) and 5.5 ± 1.5 for K_D(E–TTP)/K_D(E–dGTP). Within experimental error, these ratios agree with the ratios of 2.8 ± 1.0 and 6.8 ± 3.0, respectively, obtained by equilibrium dialysis (Englund

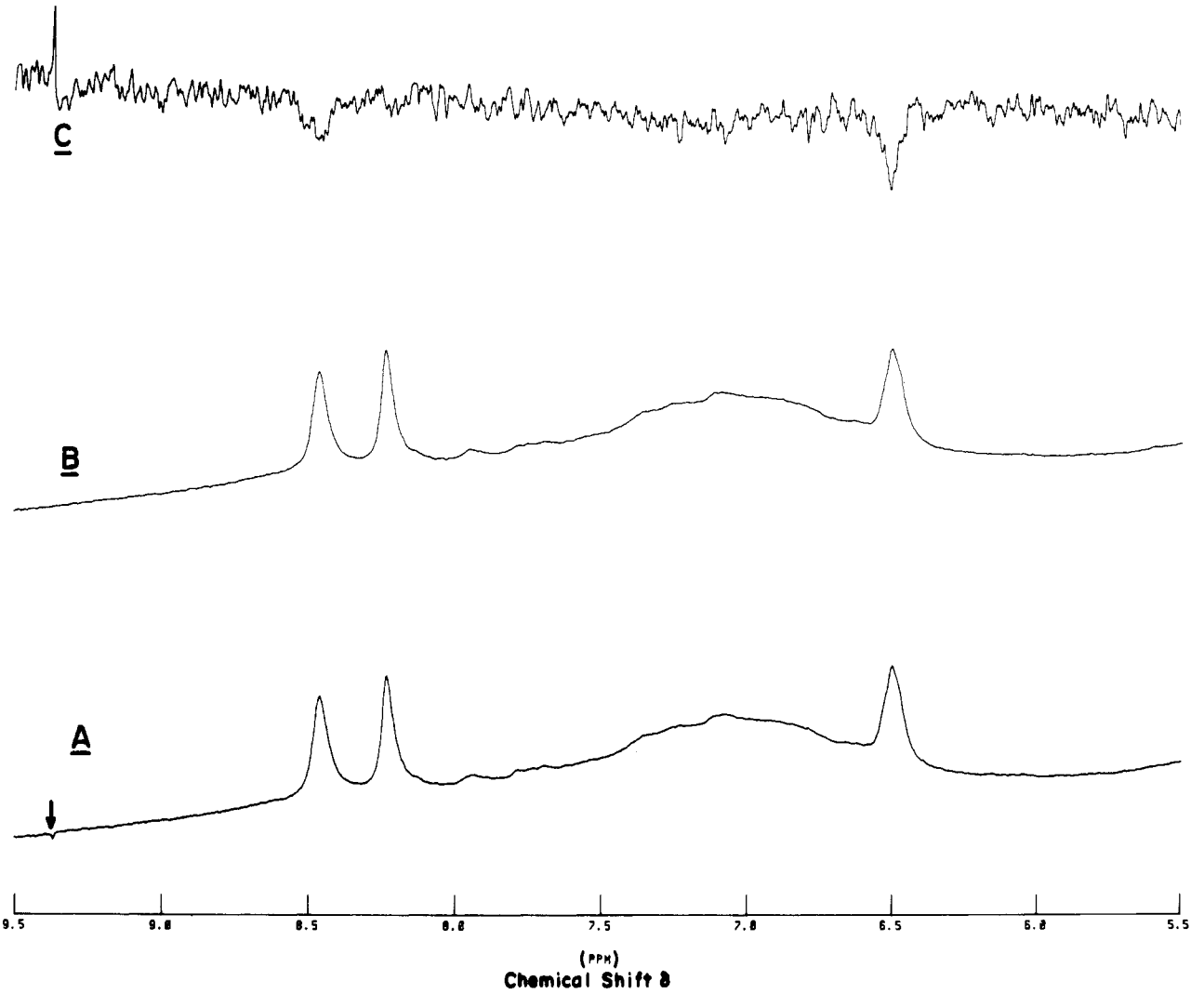

FIGURE 5: Proton NMR spectra of Mg^{2+}dATP in the presence of the large fragment of Pol I, searching for NOE's from deoxyribose H2′. The sample contained 3.38 mM dATP, 4.50 mM $MgCl_2$, and 0.157 mM large fragment. (A) The control spectrum with preirradiation at 9.37 ppm for 0.7 s. (B) Spectrum resulting from preirradiation of deoxyribose H2′ at 2.82 ppm for 0.7 s. (C) NOE difference spectrum obtained by subtracting the control spectrum A from spectrum B and increasing the vertical scale of the difference spectrum 16-fold. Spectra were acquired from 256 transients with a recycle time of 2.8 s. The preirradiation pulse power was 10 μW. A line broadening of 2 Hz was used in processing all NOE data. Other experimental and NMR parameters were as described in Figure 1.

et al., 1969), although the absolute values of the dissociation constants under the conditions of the latter experiments were (4 ± 2)-fold lower.

Similar titration studies substituting either dGMP or Mg^{2+}dGMP for the Mg^{2+}dGTP failed to detect renarrowing of Mg^{2+}TTP resonances. The failure to displace TTP by dGMP indicates substantially (>20-fold) weaker binding of monophosphates at the triphosphate site. Such behavior was also seen by equilibrium dialysis (Englund et al., 1969).

Intramolecular Nuclear Overhauser Effects on Enzyme-Bound dATP. The downfield portion of a typical 250-MHz proton NMR spectrum of Mg^{2+}dATP (3.38 mM) and large fragment (0.157 mM) is shown in Figure 5. The control spectrum (Figure 5A) was acquired with a preirradiation time of 0.7 s at 9.37 ppm, a frequency at which there are no resonances of the protein or nucleotide. Preirradiation of deoxyribose H2′ at 2.82 ppm for 0.7 s (Figure 5B) resulted in negative NOE's to adenine H8 and deoxyribose H1′ as observed in Figure 5C, obtained by subtracting spectrum A from B and increasing the gain 16-fold. In the absence of enzyme, preirradiation of the resonances of Mg^{2+}dATP, which requires a 60–200-fold greater power, gives only positive NOE's, which appear more slowly, as is generally observed for small molecules (Rosevear et al., 1983), indicating a negligible contribution of NOE's from the free substrate. This point was independently confirmed in displacement experiments with Mg^{2+}dGTP, under conditions described in the preceding section, which quantitatively eliminated the negative NOE's of enzyme-bound Mg^{2+}dATP and revealed no positive NOE's at the low power used (10 μW).

Figure 6 shows the time dependence of the NOE's from deoxyribose H2′, and their errors, in the presence of the large fragment. The primary NOE's to deoxyribose H1′ and adenine H8 appear much more rapidly than do the secondary NOE's to adenine H2. The small initial lag observed in the primary NOE's results from the time required to saturate deoxyribose H2′ and is approximated by the rate constant c in eq 1. The much longer initial lag in the secondary NOE's to adenine H2 results from the time required to transfer energy from deoxyribose H2′ to adenine H2 via intermediary spins. The primary NOE's contain distance information that is easily extracted by using eq 2. The secondary NOE's contain distance information, but extraction of the distance requires knowledge of the position of the intermediary spins (Noggle & Shirmer, 1971).

Once the time dependence of the primary NOE's $[f_A(B)_t]$

Table II: Longitudinal Relaxation Rates, Cross-Relaxation Rates, and Interproton Distances for Bound dATP[a]

proton pair (B→A)[b]	dATP bound to the large fragment[c] ρ_A (s^{-1})[e]	$-\sigma_{AB}$ (s^{-1})[f]	r_{AB} (Å)[g]	ρ_A (s^{-1})[e]	$-\sigma_{AB}$ (s^{-1})[f]	r_{AB} (Å)[g]	dATP bound to the whole Pol I[d] ρ_A (s^{-1})[e]	$-\sigma_{AB}$ (s^{-1})[f]	r_{AB} (Å)[g]
H2″→H1′	2.17	0.230	2.37	1.96	0.171	2.37	3.82	0.417	2.37
H2′→A-H8	3.11	0.143	2.57	1.92	0.125	2.50	3.61	0.211	2.65
H3′→A-H8	3.11	0.185	2.46	1.92	0.138	2.46	3.61	0.207	2.66
H5′,H5″→A-H8	3.11	0.079	2.83				3.61	0.121	2.91
H4′→H1′	2.17	0.123	2.63				3.82	0.181	2.72
H1′→H4′				1.89	0.076	2.71			
H3′→H2′				3.85	0.230	2.26	8.55	0.600	2.23
H2″→H2′[h]				3.85	0.691	1.88	8.55	1.67	1.88
H2′→H2″[h]				3.85	0.728	1.86	8.85	1.52	1.91
H2′→H1′[h]	2.17	0.156	2.53	1.96	0.107	2.56	3.82	0.251	2.58
H1′→A-H8	3.11	≤0.035	≥3.24	1.92	≤0.066	≥2.78	3.61	≤0.161	≥2.78
A-H8→H1′							3.82	≤0.159	≥2.78
H5′,H5″→A-H2	0.69	≤0.008	≥4.15				1.89	≤0.025	≥3.79
$f(\tau_r)$ (s)[i]		-7.2×10^{-10}			-5.3×10^{-10}			-1.30×10^{-9}	
τ_r (s)[i]		1.2×10^{-9}			1.1×10^{-9}			1.7×10^{-9}	
τ_r from A-H8 T_1/T_2 (s)[j]		$\leq 2.3 \times 10^{-9}$			$\leq 2.8 \times 10^{-9}$			$\leq 2.0 \times 10^{-9}$	
τ_r from A-H2 T_1/T_2 (s)[j]		$\leq 4.4 \times 10^{-9}$			$\leq 3.9 \times 10^{-9}$			$\leq 2.5 \times 10^{-9}$	

[a] ρ values were directly measured and σ values were obtained by fitting time-dependent NOE's to eq 1 as described under Methods, using c values ranging from 5.8 to 7.0 s^{-1}. [b] B refers to the irradiated resonance. A refers to the observed resonance. [c] The experiment in columns 2–4 was done at the following concentrations (mM): large fragment, 0.130; dATP, 2.75; Mg^{2+}, 3.07. The experiment in columns 5–7 was done at the following concentrations (mM): large fragment, 0.382; dATP, 16.6; Mg^{2+}, 26.4. Other components and conditions are described in Table I. [d] The experiment was done at the following concentrations (mM): whole Pol I, 0.215; dATP, 8.42; Mg^{2+}, 15.0. [e] Errors in ρ_A are typically ±5%. [f] Errors in σ_{AB} are typically ±10%. [g] Errors in ratio of distances (relative distances) are typically ±2%. Errors in absolute distances are typically ±7%. [h] Due to proximity of H2′ and H2″ resonances resulting in a mixed effect, these calculated distance values were not used in determining the conformation. [i] $f(\tau_r)$ calculated from eq 2 assuming an interproton distance between H2″ and H1′ of 2.37 ± 0.1 Å. τ_r calculated from eq 3. [j] Upper limit correlation times (τ_r) determined from T_1/T_2 ratios using eq 4.

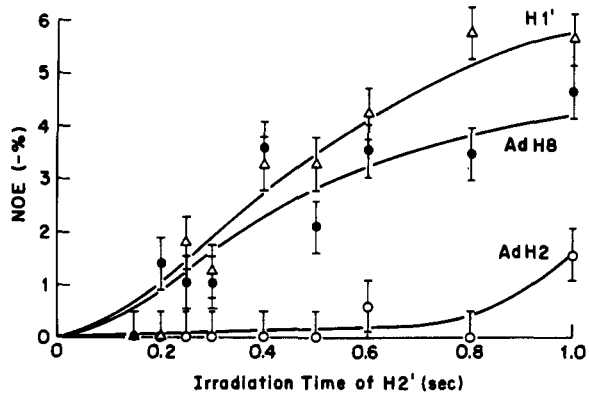

FIGURE 6: Time dependence of the NOE's to adenine H8, adenine H2, and deoxyribose H1′ upon preirradiation of deoxyribose H2′. The two upper curves represent theoretical fits to the primary NOE's with eq 1 using $c = 5.8$ s^{-1} and the parameters given in Table II. The lower curve represents a secondary NOE from deoxyribose H2′ to adenine H2. The sample contained 2.75 mM dATP, 3.07 mM $MgCl_2$, and 0.130 mM large fragment. A recycle time of 8 s was used. Other conditions were as described in Figure 5.

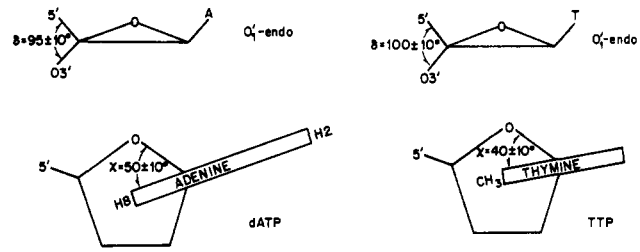

FIGURE 7: Conformations of Mg^{2+}dATP and Mg^{2+}TTP bound to the large fragment of Pol I. (Left) Conformation of Mg^{2+}dATP as determined by the distance measurements in Table II. (Right) Conformation of Mg^{2+}TTP as determined by the distance measurements in Table III.

and the longitudinal relaxation rates (ρ_A) of individual resonances were measured, cross-relaxation rates (σ_{AB}) for various pairs of spins were calculated by using eq 1. For those pairs of spins showing no primary NOE, the noise level of the NOE experiments, typically ±0.5% as estimated by spectral integration, was used to calculate the upper limit values of σ_{AB}.

As can be seen from eq 2, the ratio of any two interproton distances is equal to the inverse sixth root of the ratio of their σ_{AB} values. An absolute interproton distance requires a value for the correlation function, $f(\tau_r)$. In the present study, $f(\tau_r)$ was determined by using the distance between H2″ and H1′, which is 2.37 ± 0.1 Å for all possible deoxyribonucleotide conformations. An upper limit value of τ_r was independently calculated from the T_1/T_2 ratios by using eq 4. The values for the longitudinal relaxation rates (ρ_A), the cross-relaxation rates (σ_{AB}), the interproton distances (r_{AB}), and the calculated correlation functions and times [$f(\tau_r)$ and τ_r] are given in Table II.

As can be seen in Table II, the interproton distances of dATP bound to whole Pol I are very similar to those of dATP bound to the large fragment of Pol I. The correlation time, τ_r, is 1.4-fold larger for whole Pol I (1.7×10^{-9} s vs. 1.2×10^{-9} s) as one would expect since whole Pol I is a slightly (1.5-fold) larger protein.

Conformation of Enzyme-Bound dATP. A framework molecular model was constructed for dATP by using the calculated distances of Table II. The resulting structure thus obtained was found to be consistent with the lower limit distances as well. The final conformation of dATP bound to the large fragment of Pol I (Figure 7A) has a glycosidic torsional angle ($\chi = 50 \pm 10°$) that is clearly anti.

The H4′–H1′ interproton distance is the most important one in defining the sugar pucker since its value is 2.7 Å for O1′-endo, 3.3 Å for C3′-endo, and 3.4 Å for C2′-endo conformations (Levitt & Warshel, 1978). The measured H4′–H1′ distance of 2.7 ± 0.2 Å (Table II) indicates that enzyme-bound dATP is predominantly O1′-endo. However, satisfying all of the measured distances requires a small amount of C3′-endo character (Figure 7A). The C5′–C4′–C3′–O3′ exocyclic torsional angle, δ, provides a quantitative description of the

Table III: Longitudinal Relaxation Rates, Cross-Relaxation Rates, and Interproton Distances for TTP Bound to the Large Fragment[a]

proton pair (B→A)	ρ_A (s^{-1})	σ_{AB} (s^{-1})	r_{AB} (Å)
H2″→H1′	2.56	0.402	2.37
H2′→T-H6	3.85	0.254	2.56
H3′→T-H6	3.85	0.123	2.89
H4′→H1′	2.56	0.167	2.74
H5′,H5″→T-H6	3.85	0.102	2.98
T-H5 Me→T-H6	3.85	0.174	2.72
T-H6→T-H5 Me	2.13	0.144	2.81
H1′→T-H6	3.85	≤0.040	≥3.48
H1′→T-H5 Me	2.13	≤0.011	≥4.32
T-H6→H1′	2.56	≤0.068	≥3.19
T-H5 Me→H1′	2.56	≤0.011	≥4.32
$f(\tau_r)$ (s)		-1.25×10^{-9}	
τ_r (s)		1.6×10^{-9}	
τ_r from T-H6 T_1/T_2 (s)		$\leq 1.7 \times 10^{-9}$	
τ_r from T-H5 Me T_1/T_2 (s)		$\leq 2.0 \times 10^{-9}$	

[a] The experiment was done at the following concentrations (mM): large fragment, 0.147; TTP, 3.11; Mg^{2+}, 3.41. Other components and conditions are as described in Table II. Definitions and errors are as given in Table II. The c values ranged from 3.4 to 11.2 s^{-1}.

sugar pucker (Levitt & Warshel, 1978; Dickerson et al., 1982). For dATP bound to the large fragment, $\delta = 95 \pm 10°$, and this angle also identifies the sugar pucker as predominantly O1′-endo. Within experimental error, the conformation of dATP bound to whole Pol I, on the basis of the distances in Table II, is indistinguishable from that found on the large fragment.

Conformation of Enzyme-Bound TTP. The same conditions and techniques and control displacements with Mg^{2+}dGTP used to determine the conformation of dATP bound to the large fragment were applied to TTP. However, in the case of TTP bound to large fragment, the overlapping H2′ and H2″ resonances at 2.37 ppm (Figure 2) were simultaneously irradiated, so a 20% subtraction was applied to the observed cross-relaxation rate between the H2′ and H2″ spins and the H1′ spin to obtain a pure value for $\sigma_{H2''\rightarrow H1'}$. For all conformations of deoxyribonucleotides, H2″ is much closer than H2′ to H1′ (Levitt & Warshel, 1978), and the contribution (using eq 2) due to $\sigma_{H2'\rightarrow H1'}$ could only be 20 ± 5%. This uncertainty in the $\sigma_{H2'\rightarrow H1'}$ contribution to the observed cross-relaxation rate could result in a maximal error of only ±0.03 Å in the calculated distance between H2″ and H1′.

The results obtained for TTP bound to the large fragment (Table III) are similar to those obtained for bound dATP (Table II). The molecular model constructed for bound TTP (Figure 7B) had an anti-glycosidic torsional angle, χ, of 40 ± 10° and an O1′-endo pucker with $\delta = 100 \pm 10°$.

Intermolecular Nuclear Overhauser Effects from Enzyme to Substrates. Figures 8 and 9 show NOE action spectra resulting from irradiation throughout the proton NMR spectrum of the large fragment of Pol I on the intensities of the resonances of dATP and TTP, respectively. Several distinct peaks in the action spectra are noted as well as regions of the proton spectrum that, upon irradiation, produced no effects. Such selective effects argue against a significant contribution of nonspecific spin–diffusion to the observed NOE's (Kalk & Berendsen, 1976) and indicate the proximity (i.e., within 5 Å) of several amino acid protons to those of the bound substrates. The NOE's to adenine H8 and H2 and deoxyribose H1′ of dATP from the aliphatic region of the proton NMR spectrum (Figure 8) occur at differing chemical shifts requiring the contribution of more than one hydrophobic amino acid side chain. While two Ile residues with differing ring current shifts, or an Ile + Leu pair, would provide the

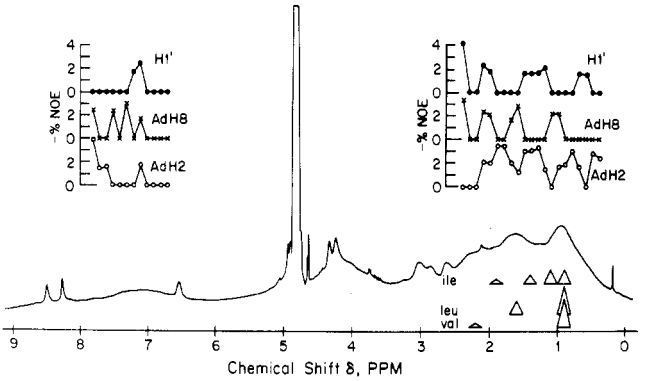

FIGURE 8: NOE action spectra from the large fragment of Pol I to protons of Mg^{2+}dATP. A control spectrum of the enzyme, Mg^{2+}, and dATP is shown below, as are the approximate positions and line widths of Ile, Leu, and Val residues. The preirradiation pulse, as described under Experimental Procedures, had a power of 20 μW and a duration of 1.0 s. Other conditions were as described in Figures 5 and 6.

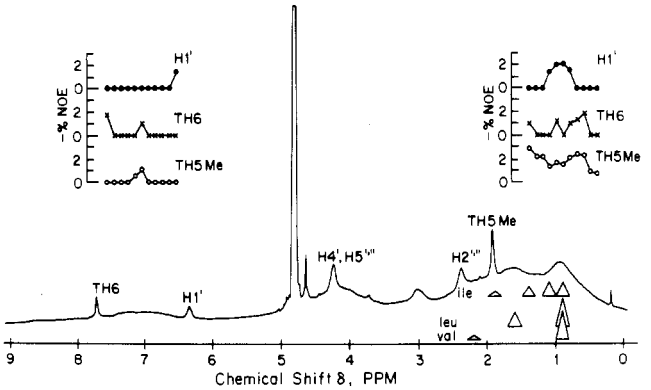

FIGURE 9: NOE action spectra from the large fragment of Pol I to protons of Mg^{2+}TTP. The sample contained 3.11 mM TTP, 3.41 mM $MgCl_2$, and 0.147 mM large fragment. A control spectrum of the enzyme, Mg^{2+}, and TTP is shown below as are the approximate positions and line widths of Ile, Leu, and Val residues. Other conditions are as described in Figures 5, 6, and 8.

simplest explanation of the observed NOE's (Figure 8) combinations of more than two other hydrophobic residues such as Leu + Val cannot be excluded. In addition, a number of other residues could contribute to the NOE's between 1.4 and 2.1 ppm. The NOE's from 7.1–7.3 ppm to bound dATP indicate the proximity of an aromatic residue (Tyr, Phe, His, or Trp) to the bound substrate. Similarly, the NOE's to bound TTP indicate the proximity of both hydrophobic (0.6–0.9 ppm) and aromatic residues (7.0 ppm) to the bound substrate. NOE's from the aliphatic region could not be investigated in greater detail with TTP due to overlap of the thymine H5 methyl resonance.

Discussion

Two major lines of evidence indicate that the deoxynucleoside triphosphates are bound to Pol I and its large fragment. First, the concentration dependence of the line-broadening effect of the enzymes on the deoxyribonucleoside triphosphate proton resonances and the competitive removal of these effects by Mg^{2+}dGTP argue for binding to the single triphosphate site detected on whole Pol I by Englund et al. (1969). Second, the interproton NOE's of the deoxynucleoside triphosphate substrates change in sign from positive to negative in the presence of Pol I or its large fragment, indicating an increase in the rotational correlation time (τ_r) of the substrates. As may be seen in eq 2 and 3, the enhancement observed with

a rapidly rotating small ligand, such as dATP, occurs because $\omega_I\tau_r < 1.12$ ($\tau_r < 7 \times 10^{-10}$ s), while a decrease in intensity is observed in the case of enzyme-bound dATP where $\omega_I\tau_r > 1.12$ ($\tau_r > 7 \times 10^{-10}$ s).

The interproton distances based on the present NOE measurements (Tables II and III) greatly extend our knowledge of the detailed conformations of the bound substrates of Pol I (Figure 7). Earlier studies in this laboratory of the conformations of Mn^{2+}dATP and Mn^{2+}TTP bound to whole Pol I (Sloan et al., 1975) involved measuring the paramagnetic effects of enzyme-bound Mn^{2+} on the longitudinal relaxation rates of the deoxynucleoside triphosphate proton and phosphorous resonances. Mn^{2+} to proton and Mn^{2+} to phosphorus distances were measured, and glycosidic torsional angles of $90 \pm 10°$ were estimated for both Mn^{2+}dATP and Mn^{2+}TTP bound to whole Pol I. A syn conformation for bound dATP could not be excluded, and no conclusions as to sugar pucker could be drawn since too few conformationally sensitive Mn^{2+}–proton distances were measurable. The discrepancy in χ values based on the early paramagnetic study and the present NOE measurements was resolved when it was realized that in the paramagnetic study, carried out at a lower frequency, the overlapping H4′, H5′, and H5″ resonances were misassigned only to H4′. Correction of the assignment resulted in conformations of Mn^{2+}dATP and Mn^{2+}TTP indistinguishable from those established in the present study (Figure 7). The mutual consistency between the substrate conformations based on the corrected Mn^{2+}–proton distances and the present interproton distances argues cogently for unique substrate conformations on Pol I.

The anti-glycosidic torsional angles (χ) determined in the present studies are well within the range seen in crystallographic studies of deoxyribofuranoside derivatives (de Leeuw et al., 1980). The crystallographic structure of 5′-dAMP has $\chi = 64°$ with a C2′-endo, C3′-endo deoxyribose (Reddy & Viswamitra, 1975) and 5′-TMP has $\chi = 43°$ with a C3′-endo deoxyribose (Trueblood et al., 1961).

The O1′-endo sugar pucker of the two bound deoxyribonucleoside triphosphates is not a common feature in crystallographically determined structures, but it is certainly precedented. For example, an O1′-endo sugar pucker has been seen in the crystal structures of dGMP (Viswamitra & Seshadri, 1974; Young et al., 1974), 1-β-D-arabinofuranosylthymine (Tougard et al., 1973), (−)-(5*S*)-5-hydroxy-5,6-dihydrothymidine (Grand & Cadet, 1978), dihydrothymidine (Konnert et al., 1970), and 5-iodo-5′-amino-2′,5′-dideoxyuridine (Birnbaum et al., 1979) and in the B-DNA dodecamer CGCGAATTCGCG (Dickerson et al., 1982). Theoretical calculations indicate O1′-endo is only about 0.6 kcal/mol higher in energy than C2′-endo or C3′-endo (Levitt & Warshel, 1978), although more recent calculations indicate that O1′-endo is 1.8 kcal/mol higher in energy (Olson, 1982). A recent conformational study of tetraamminecobalt^{III}–ATP bound to the catalytic subunit of bovine heart protein kinase has suggested an O1′-endo ribose with a $\chi = 78 \pm 10°$ (Rosevear et al., 1983).

Previous studies from this laboratory had suggested that DNA polymerase holds substrates in a conformation like that of an average deoxynucleotidyl unit of B DNA, as determined by X-ray fiber diffraction (Arnott & Hukins, 1969), and that this effect might contribute to the high fidelity of the polymerase reaction in copying templates (Sloan et al., 1975). The present refined and more detailed information on the conformations of the bound substrates, together with the recently obtained high-resolution single-crystal X-ray structures of various forms of DNA (Dickerson et al., 1982; Wang et al., 1981), permits a more critical test of this idea.

The conformations of bound Mg^{2+}dATP ($\chi = 50 \pm 10°$, $\delta = 95 \pm 10°$) and bound Mg^{2+}TTP ($\chi = 40 \pm 10°$, $\delta = 100 \pm 10°$) are compared to the χ and δ values found in A, B, and Z DNAs in the diagrams of Figure 10. The χ and δ values for bound Mg^{2+}dATP and bound Mg^{2+}TTP fall in the lower range of those seen for B DNA (Figure 10, middle), somewhat above the range for A DNA (Figure 10, top), and totally outside the range seen for Z DNA (Figure 10, bottom) (Dickerson et al., 1982).

The difference between the conformations of nucleotides bound to Pol I and Z DNA is especially striking. In Z DNA the purine glycosidic torsional angle is in the syn range, while Mg^{2+}dATP bound to Pol I is clearly anti. In addition, the Z-DNA pyrimidine deoxyribose moieties cluster tightly around the C2′-endo conformations, while Mg^{2+}TTP bound to Pol I has a O1′-endo conformation. As previously noted (Dickerson et al., 1982; Sundaralingam, 1973), there is a linear correlation between χ and δ for deoxynucleotide units of B DNA. Nucleotide units with an O1′-endo sugar pucker have lower glycosidic torsional angles than do units with C2′-endo sugar puckers. The conformations of Mg^{2+}dATP and Mg^{2+}TTP bound to Pol I fall on this linear correlation between χ and δ and thus are consistent with the hypothesis of prealignment of the deoxynucleoside triphosphate in a B-DNA-like conformation prior to polymerization. This view will be further documented in a study of substrate conformations in the presence of bound template and in a study of the conformation of the bound template (Ferrin & Mildvan, 1984).

The NOE's seen on the resonances of dATP and TTP produced by irradiation of protein resonances (Figures 8 and 9) were used to assess the nature of amino acid residues near the triphosphate binding site. The chemical shifts at the maxima of the action spectra were compared to the chemical shifts of amino acid residues in a random-coil protein, which are believed to be accurate to within 0.3 ppm (Wuthrich, 1976).

The simplest explanation of the NOE action spectra is that two hydrophobic amino acids, at least one of which is an Ile, as well as an aromatic amino acid, interact with the bound substrates. However, more complicated interpretations cannot as yet be excluded. Thus, NOE's from the protein to adenine H2, thymine H6, thymine H5 methyl, and deoxyribose H1′ of dATP were observed at chemical shifts <0.8 ppm. Such effects in the aliphatic region of the enzyme could arise only from irradiation of one or more methyl groups of hydrophobic amino acids as Ile, Leu, or Val. The maxima seen in the region of 0.9–2.1 ppm are more difficult to interpret, since several residues absorb in this region. Isoleucine, which absorbes at 0.9 ppm (δ-CH_3), 1.1 ppm (γ-CH_3), 1.4 ppm (γ-CH_2), and 1.9 ppm (β-CH), is the only residue that absorbs within 0.3 ppm of all the maxima seen in the aliphatic region, but several combinations of two or more residues could be responsible for these effects. A further observation that the positions of the maxima to different deoxyribonucleoside triphosphate resonances do not coincide (Figures 8 and 9) indicates that more than one hydrophobic amino acid is in close proximity to the triphosphate site. The effects seen at 7.0–7.3 ppm could arise only from irradiation of one or more ring protons of an aromatic amino acid such as Tyr, Trp, His, or Phe. However, the action spectra measured at a shorter preirradiation time (0.5 instead of 1.0 s, data not shown) indicated that aromatic residues are more distant from the substrates than the aliphatic hydrophobic ones.

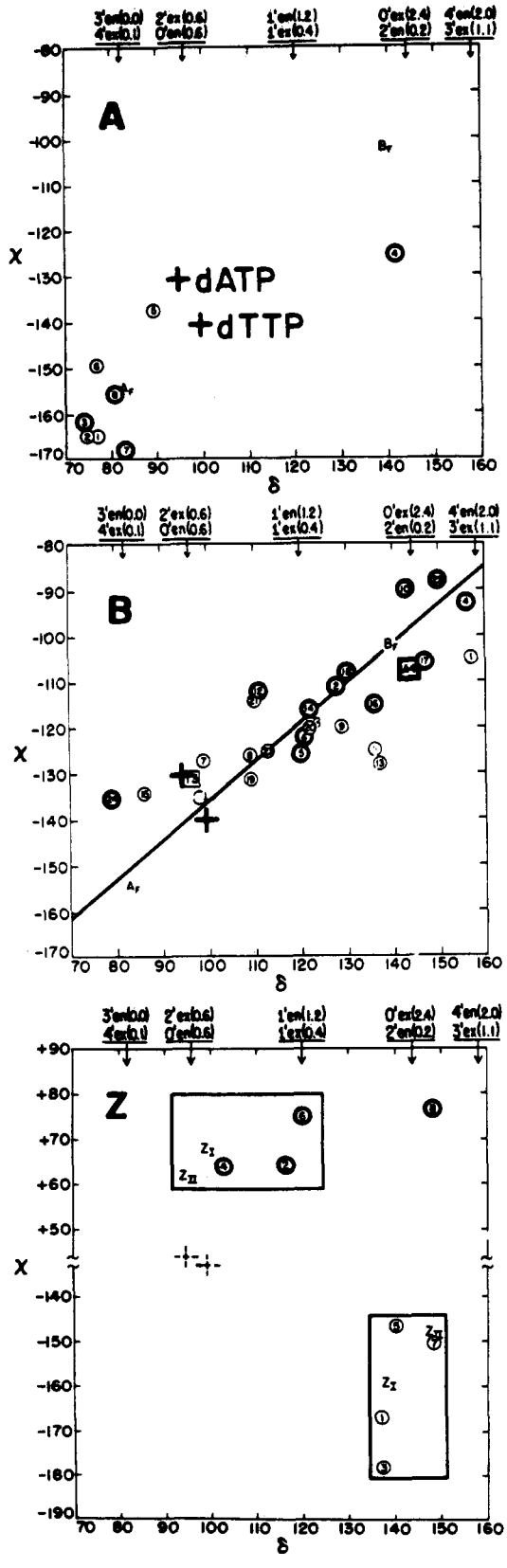

FIGURE 10: Conformation plot of glycosidic torsional angles (χ) vs. deoxyribose C3′–C4′ dihedral angles (δ) in A, B, and Z DNA determined crystallographically and of Mg^{2+}dATP and Mg^{2+}TTP bound to the large fragment of Pol I. The diagrams are modified from a review by Dickerson et al. (1982). Dickerson's definition of χ differs from ours by −180°. (Top) Dihedral angles found in the A-DNA tetramer CCGG. (Middle) Angles found in the B-DNA dodecamer CGCGAATTCGCG. (Bottom) Angles found in the high-salt Z-DNA tetramer CGCG. The crosses show the dihedral angles of Mg^{2+}dATP and Mg^{2+}TTP. The solid line in (B) shows the linear correlation between χ and δ characteristic of B DNA.

The presence of Ile, Leu, or Val near nucleoside triphosphate binding sites has also been detected by analogous NOE measurements on ATP bound to adenylate kinase (Smith & Mildvan, 1982) and creatine kinase (James, 1976; Vasak et al., 1979).

ACKNOWLEDGMENTS

We are grateful to Drs. William Brown and John Bodner for providing us with *E. coli* strain CM5199 and for advice in the purification of Pol I, to Drs. Nigel Grindley and Catherine Joyce for providing us with *E. coli* strain CJ155 and for helpful discussions, and to Dr. Lawrence A. Loeb for helpful advice.

REFERENCES

Arnott, S., & Hukins, D. W. L. (1969) *Nature (London) 224*, 886.

Birnbaum, G. I., Lin, T., Shiau, G. T., & Prusoff, W. H. (1979) *J. Am. Chem. Soc. 101*, 3353.

Brutlag, D., Atkinson, M. R., Setlow, P., & Kornberg, A. (1969) *Biochem. Biophys. Res. Commun. 37*, 982.

de Leeuw, H. P. M., Haasnoot, C. A. G., & Altona, C. (1980) *Isr. J. Chem. 20*, 108.

Dickerson, R. E., Drew, H. R., Conner, B. N., Wing, R. M., Fratini, A. V., & Kopka, M. L. (1982) *Science (Washington, D.C.) 216*, 475.

Englund, P. T., Huberman, J. A., Jovin, T. M., & Kornberg, A. (1969) *J. Biol. Chem. 244*, 3038.

Ferrin, L. J., & Mildvan, A. S. (1984) *Fed. Proc., Fed. Am. Soc. Exp. Biol. 43*, 1539 (Abstr.).

Ferrin, L. J., & Mildvan, A. S. (1985) *Biophys. J. 47*, 389a (Abstr.).

Ferrin, L. J., Mildvan, A. S., & Loeb, L. A. (1983) *Biochem. Biophys. Res. Commun. 112*, 723.

Grand, A., & Cadet, J. (1978) *Acta Crystallogr., Sect. B: Struct. Crystallogr. Cryst. Chem. B34*, 1524.

James, T. L. (1976) *Biochemistry 15*, 4724.

Jovin, T. M., Englund, P. T., & Bertsch, L. L. (1969) *J. Biol. Chem. 244*, 2996.

Joyce, C. M., & Grindley, N. D. F. (1983) *Proc. Natl. Acad. Sci. U.S.A. 80*, 1830.

Joyce, C. M., Kelley, W. S., & Grindley, N. D. F. (1982) *J. Biol. Chem. 257*, 1958.

Kalk, A., & Berendsen, H. J. C., (1976) *J. Magn. Reson. 24*, 343.

Kelley, W. S., & Stump, K. H. (1979) *J. Biol. Chem. 254*, 3206.

Kerson, L. A., Garfinkel, D., & Mildvan, A. S. (1967) *J. Biol. Chem. 242*, 2124.

Klenow, H., & Henningsen, I. (1970) *Proc. Natl. Acad. Sci. U.S.A. 65*, 168.

Konnert, J., Karle, I. L., & Karle, J. (1970) *Acta Crystallogr., Sect. B: Struct. Crystallogr. Cryst. Chem. B26*, 770.

Kornberg, A. (1980) *DNA Replication*, W. H. Freeman, San Francisco.

Kornberg, A. (1982) *1982 Supplement to DNA Replication*, W. H. Freeman, San Francisco.

Levitt, M., & Warshel, A. (1978) *J. Am. Chem. Soc. 100*, 2607.

Lowry, O. H., Rosebrough, N. J., Farr, A. L., & Randall, R. J. (1951) *J. Biol. Chem. 193*, 265.

Noggle, J. H., & Schirmer, R. E. (1971) *The Nuclear Overhauser Effect*, Academic Press, New York.

Ollis, D. L., Brick, P., Hamlin, R., Xuong, N. G., & Steitz, T. A. (1985) *Nature (London) 313*, 762.

Olson, W. K. (1982) *J. Am. Chem. Soc. 104*, 278.

Reddy, B. S., & Viswamitra, M. A. (1975) *Acta Crystallogr., Sect. B: Struct. Crystallogr. Cryst. Chem. B31*, 19.
Rosevear, P. R., Bramson, H. N., O'Brian, C., Kaiser, E. T., & Mildvan, A. S. (1983) *Biochemistry 22*, 3439.
Schmidt, P. G., Stark, G. R., & Baldeschwieler, J. D. (1969) *J. Biol. Chem. 244*, 1860.
Setlow, P. (1974) *Methods Enzymol. 29*, 3.
Setlow, P., Brutlag, D., & Kornberg, A. (1972) *J. Biol. Chem. 247*, 224.
Sloan, D. L., Loeb, L. A., Mildvan, A. S., & Feldman, R. J. (1975) *J. Biol. Chem. 250*, 8913.
Smith, G. M., & Mildvan, A. S. (1982) *Biochemistry 21*, 6119.
Solomon, I. (1955) *Phys. Rev. 99*, 559.
Sundaralingam, M. (1973) *Jerusalem Symp. Quantum Chem. Biochem. 5*, 417.
Tougard, P. P. (1973) *Acta Crystallogr., Sect. B: Struct. Crystallogr. Cryst. Chem. B29*, 2227.
Travaglini, E. C., Mildvan, A. S., & Loeb, L. A. (1975) *J. Biol. Chem. 250*, 8647.
Tropp, J. (1980) *J. Chem. Phys. 72*, 6035.
Trueblood, K. N., Horn, P., & Luzzati, V. (1961) *Acta Crystallogr. 14*, 965.
Vasak, M., Nagayama, K., Wuthrich, K., Mertens, M. L., & Kagi, J. H. R. (1979) *Biochemistry 18*, 5050.
Viswamitra, M. A., & Seshadri, T. P. (1974) *Nature (London) 252*, 176.
Wagner, G., & Wuthrich, K. (1979) *J. Magn. Reson. 33*, 675.
Wang, A. H.-J., Quigley, G. J., Kolpak, F. J., van der Marel, G., van Boom, J. H., & Rich, A. (1981) *Science (Washington, D.C.) 211*, 171.
Wuthrich, K. (1976) *NMR in Biological Research: Peptides and Proteins*, American Elsevier, New York.
Young, D. W., Tollin, P., & Wilson, H. R. (1974) *Acta Crystallogr., Sect. B.: Struct. Crystallogr. Cryst. Chem. B30*, 2012.

Mode of Reversible Binding of Neocarzinostatin Chromophore to DNA: Evidence for Binding via the Minor Groove†

Dipak Dasgupta and Irving H. Goldberg*
Department of Pharmacology, Harvard Medical School, Boston, Massachusetts 02115
Received May 3, 1985

ABSTRACT: Two general approaches have been taken to understand the mechanism of the reversible binding of the nonprotein chromophore of neocarzinostatin to DNA: (1) measurement of the relative affinity of the chromophore for various DNAs that have one or both grooves blocked by bulky groups and (2) studies on the influence of adenine–thymine residue-specific, minor groove binding agents such as the antibiotics netropsin and distamycin on the chromophore–DNA interaction. Experiments using synthetic DNAs containing halogen group (Br, I) substituents in the major groove or natural DNAs with glucosyl moieties projecting into the major groove show that obstruction of the major groove does not decrease the binding stoichiometry or the binding constant for the DNA–chromophore interaction. Chemical methylation of bases in both grooves of calf thymus DNA, resulting in 13% methylation of N-7 of guanine in the major groove and 7% methylation of N-3 of adenine in the minor groove, decreases the binding affinity and increases the size of the binding site for neocarzinostatin chromophore. Similar results were obtained whether binding parameters were determined directly by spectroscopic measurements or indirectly by measuring the ability of the DNA to protect the chromophore against degradation. On the other hand, netropsin and distamycin compete with neocarzinostatin chromophore for binding to the minor groove of DNA, as shown by their decrease in the ability of poly(dA-dT) to protect the chromophore against degradation and their reduction in chromophore-induced DNA damage as measured by thymine release. Taken together with earlier evidence that neocarzinostatin chromophore intercalates DNA, these data support a binding model in which the naphthoic acid moiety of neocarzinostatin chromophore intercalates between the base pairs of DNA by way of its minor groove.

The nonprotein chromophore of the DNA-damaging antibiotic neocarzinostatin [reviewed in Goldberg et al. (1981)] binds reversibly to helical DNA in the absence of sulfhydryl activating agents (Povirk & Goldberg, 1980; Povirk et al., 1981). Physicochemical studies on the reversible binding have shown two features: (i) the chromophore has a preferred affinity for A-T base pairs over G-C base pairs (Poon et al., 1977; Povirk & Goldberg, 1980); and (ii) it binds to natural DNA by intercalation (Povirk et al., 1981). The intercalative mode of binding has been suggested by the hydrodynamic and electric dichroic properties of the DNA–chromophore complex. The complete structure of the chromophore has been reported recently. It consists of four parts: 2-hydroxy-7-methoxy-5-methyl-1-naphthoate and 2,6-dideoxy-2-(methylamino)-galactose linked to a $C_{15}H_8O_4$ substituent consisting of an ethylene cyclic carbonate group, and a highly strained ether epoxide attached to a novel bicyclo[7.3.0]dodecadiyne system (Hensens et al., 1983; Shibuya et al., 1984; Edo et al., 1985). By analogy with other intercalators, one can a priori predict the planar naphthalene aromatic ring system to be the potential

†This work was supported by U.S. Public Health Service Grant GM 12573 from the National Institutes of Health and by an award from the Bristol-Myers Co.

0006-2960/85/0424-6913$01.50/0